Measurement of High-p_T Single Electrons from Heavy-Flavor Decays in $p + p$ Collisions at $\sqrt{s} = 200$ GeV

A. Adare,[8] S. Afanasiev,[22] C. Aidala,[9] N. N. Ajitanand,[48] Y. Akiba,[42,43] H. Al-Bataineh,[37] J. Alexander,[48] K. Aoki,[27,42] L. Aphecetche,[50] R. Armendariz,[37] S. H. Aronson,[3] J. Asai,[43] E. T. Atomssa,[28] R. Averbeck,[49] T. C. Awes,[38] B. Azmoun,[3] V. Babintsev,[18] G. Baksay,[14] L. Baksay,[14] A. Baldisseri,[11] K. N. Barish,[4] P. D. Barnes,[30] B. Bassalleck,[36] S. Bathe,[4] S. Batsouli,[38] V. Baublis,[41] A. Bazilevsky,[3] S. Belikov,[3] R. Bennett,[49] Y. Berdnikov,[45] A. A. Bickley,[8] J. G. Boissevain,[30] H. Borel,[11] K. Boyle,[49] M. L. Brooks,[30] H. Buesching,[3] V. Bumazhnov,[18] G. Bunce,[3,43] S. Butsyk,[30,49] S. Campbell,[49] B. S. Chang,[57] J.-L. Charvet,[11] S. Chernichenko,[18] J. Chiba,[23] C. Y. Chi,[9] M. Chiu,[19] I. J. Choi,[57] T. Chujo,[54] P. Chung,[48] A. Churyn,[18] V. Cianciolo,[38] C. R. Cleven,[16] B. A. Cole,[9] M. P. Comets,[39] P. Constantin,[30] M. Csanád,[13] T. Csörgő,[24] T. Dahms,[49] K. Das,[15] G. David,[3] M. B. Deaton,[1] K. Dehmelt,[14] H. Delagrange,[50] A. Denisov,[18] D. d'Enterria,[9] A. Deshpande,[43,49] E. J. Desmond,[3] O. Dietzsch,[46] A. Dion,[49] M. Donadelli,[46] O. Drapier,[28] A. Drees,[49] A. K. Dubey,[56] A. Durum,[18] V. Dzhordzhadze,[4] Y. V. Efremenko,[38] J. Egdemir,[49] F. Ellinghaus,[8] W. S. Emam,[4] A. Enokizono,[29] H. En'yo,[42,43] S. Esumi,[53] K. O. Eyser,[4] D. E. Fields,[36,43] M. Finger, Jr.,[5,22] F. Fleuret,[28] S. L. Fokin,[26] Z. Fraenkel,[56] A. Franz,[3] J. Frantz,[49] A. D. Frawley,[15] K. Fujiwara,[42] Y. Fukao,[27,42] T. Fusayasu,[35] S. Gadrat,[31] I. Garishvili,[51] A. Glenn,[8] H. Gong,[49] M. Gonin,[28] J. Gosset,[11] Y. Goto,[42,43] R. Granier de Cassagnac,[28] N. Grau,[21] S. V. Greene,[54] M. Grosse Perdekamp,[19,43] T. Gunji,[7] H.-Å. Gustafsson,[32] T. Hachiya,[17] A. Hadj Henni,[50] C. Haegemann,[36] J. S. Haggerty,[3] H. Hamagaki,[7] R. Han,[40] H. Harada,[17] E. P. Hartouni,[29] K. Haruna,[17] E. Haslum,[32] R. Hayano,[7] M. Heffner,[29] T. K. Hemmick,[49] T. Hester,[4] X. He,[16] H. Hiejima,[19] J. C. Hill,[21] R. Hobbs,[36] M. Hohlmann,[14] W. Holzmann,[48] K. Homma,[17] B. Hong,[25] T. Horaguchi,[42,52] D. Hornback,[51] T. Ichihara,[42,43] K. Imai,[27,42] M. Inaba,[53] Y. Inoue,[44,42] D. Isenhower,[1] L. Isenhower,[1] M. Ishihara,[42] T. Isobe,[7] M. Issah,[48] A. Isupov,[22] B. V. Jacak,[49] J. Jia,[9] J. Jin,[9] O. Jinnouchi,[43] B. M. Johnson,[3] K. S. Joo,[34] D. Jouan,[39] F. Kajihara,[7] S. Kametani,[7,55] N. Kamihara,[42] J. Kamin,[49] M. Kaneta,[43] J. H. Kang,[57] H. Kanou,[42,52] H. Kano,[42] D. Kawall,[43] A. V. Kazantsev,[26] A. Khanzadeev,[41] J. Kikuchi,[55] D. H. Kim,[34] D. J. Kim,[57] E. Kim,[47] E. Kinney,[8] A. Kiss,[13] E. Kistenev,[3] A. Kiyomichi,[42] J. Klay,[29] C. Klein-Boesing,[33] L. Kochenda,[41] V. Kochetkov,[18] B. Komkov,[41] M. Konno,[53] D. Kotchetkov,[4] A. Kozlov,[56] A. Král,[10] A. Kravitz,[9] J. Kubart,[5,20] G. J. Kunde,[30] N. Kurihara,[7] K. Kurita,[44,42] M. J. Kweon,[25] Y. Kwon,[51,57] G. S. Kyle,[37] R. Lacey,[48] Y.-S. Lai,[9] J. G. Lajoie,[21] A. Lebedev,[21] D. M. Lee,[30] M. K. Lee,[57] T. Lee,[47] M. J. Leitch,[30] M. A. L. Leite,[46] B. Lenzi,[46] T. Liška,[10] A. Litvinenko,[22] M. X. Liu,[30] X. Li,[6] B. Love,[54] D. Lynch,[3] C. F. Maguire,[54] Y. I. Makdisi,[3] A. Malakhov,[22] M. D. Malik,[36] V. I. Manko,[26] Y. Mao,[40,42] L. Mašek,[5,20] H. Masui,[53] F. Matathias,[9] M. McCumber,[49] P. L. McGaughey,[30] Y. Miake,[53] P. Mikeš,[5,20] K. Miki,[53] T. E. Miller,[54] A. Milov,[49] S. Mioduszewski,[3] M. Mishra,[2] J. T. Mitchell,[3] M. Mitrovski,[48] A. Morreale,[4] D. P. Morrison,[3] T. V. Moukhanova,[26] D. Mukhopadhyay,[54] J. Murata,[44,42] S. Nagamiya,[23] Y. Nagata,[53] J. L. Nagle,[8] M. Naglis,[56] I. Nakagawa,[42,43] Y. Nakamiya,[17] T. Nakamura,[17] K. Nakano,[42,52] J. Newby,[29] M. Nguyen,[49] B. E. Norman,[30] A. S. Nyanin,[26] E. O'Brien,[3] S. X. Oda,[7] C. A. Ogilvie,[21] H. Ohnishi,[42] H. Okada,[27,42] K. Okada,[43] M. Oka,[53] O. O. Omiwade,[1] A. Oskarsson,[32] M. Ouchida,[17] K. Ozawa,[7] R. Pak,[3] D. Pal,[54] A. P. T. Palounek,[30] V. Pantuev,[49] V. Papavassiliou,[37] J. Park,[47] W. J. Park,[25] S. F. Pate,[37] H. Pei,[21] J.-C. Peng,[19] H. Pereira,[11] V. Peresedov,[22] D. Yu. Peressounko,[26] C. Pinkenburg,[3] M. L. Purschke,[3] A. K. Purwar,[30] H. Qu,[16] J. Rak,[36] A. Rakotozafindrabe,[28] I. Ravinovich,[56] K. F. Read,[38,51] S. Rembeczki,[14] M. Reuter,[49] K. Reygers,[33] V. Riabov,[41] Y. Riabov,[41] G. Roche,[31] A. Romana,[28,*] M. Rosati,[21] S. S. E. Rosendahl,[32] P. Rosnet,[31] P. Rukoyatkin,[22] V. L. Rykov,[42] B. Sahlmueller,[33] N. Saito,[27,42,43] T. Sakaguchi,[3] S. Sakai,[53] H. Sakata,[17] V. Samsonov,[41] S. Sato,[23] S. Sawada,[23] J. Seele,[8] R. Seidl,[19] V. Semenov,[18] R. Seto,[4] D. Sharma,[56] I. Shein,[18] A. Shevel,[41,48] T.-A. Shibata,[42,52] K. Shigaki,[17] M. Shimomura,[53] K. Shoji,[27,42] A. Sickles,[49] C. L. Silva,[46] D. Silvermyr,[38] C. Silvestre,[11] K. S. Sim,[25] C. P. Singh,[2] V. Singh,[2] S. Skutnik,[21] M. Slunečka,[5,22] A. Soldatov,[18] R. A. Soltz,[29] W. E. Sondheim,[30] S. P. Sorensen,[51] I. V. Sourikova,[3] F. Staley,[11] P. W. Stankus,[38] E. Stenlund,[32] M. Stepanov,[37] A. Ster,[24] S. P. Stoll,[3] T. Sugitate,[17] C. Suire,[39] J. Sziklai,[24] T. Tabaru,[43] S. Takagi,[53] E. M. Takagui,[46] A. Taketani,[42,43] Y. Tanaka,[35] K. Tanida,[42,43] M. J. Tannenbaum,[3] A. Taranenko,[48] P. Tarján,[12] T. L. Thomas,[36] M. Togawa,[27,42] A. Toia,[49] J. Tojo,[42] L. Tomášek,[20] H. Torii,[42] R. S. Towell,[1] V-N. Tram,[28] I. Tserruya,[56] Y. Tsuchimoto,[17] C. Vale,[21] H. Valle,[54] H. W. van Hecke,[30] J. Velkovska,[54] R. Vertesi,[12] A. A. Vinogradov,[26] M. Virius,[10] V. Vrba,[20] E. Vznuzdaev,[41] M. Wagner,[27,42] D. Walker,[49] X. R. Wang,[37] Y. Watanabe,[42,43] J. Wessels,[33] S. N. White,[3] D. Winter,[9] C. L. Woody,[3] M. Wysocki,[8] W. Xie,[43] Y. Yamaguchi,[55] A. Yanovich,[18] Z. Yasin,[4] J. Ying,[16] S. Yokkaichi,[42,43] G. R. Young,[38] I. Younus,[36] I. E. Yushmanov,[26] W. A. Zajc,[9,†] O. Zaudtke,[33] C. Zhang,[38] S. Zhou,[6] J. Zimányi,[24] and L. Zolin[22]

(PHENIX Collaboration)

[1]*Abilene Christian University, Abilene, Texas 79699, USA*
[2]*Department of Physics, Banaras Hindu University, Varanasi 221005, India*
[3]*Brookhaven National Laboratory, Upton, New York 11973-5000, USA*
[4]*University of California - Riverside, Riverside, California 92521, USA*
[5]*Charles University, Ovocný trh 5, Praha 1, 116 36, Prague, Czech Republic*
[6]*China Institute of Atomic Energy (CIAE), Beijing, People's Republic of China*
[7]*Center for Nuclear Study, Graduate School of Science, University of Tokyo, 7-3-1 Hongo, Bunkyo, Tokyo 113-0033, Japan*
[8]*University of Colorado, Boulder, Colorado 80309, USA*
[9]*Columbia University, New York, New York 10027, USA and Nevis Laboratories, Irvington, New York 10533, USA*
[10]*Czech Technical University, Zikova 4, 166 36 Prague 6, Czech Republic*
[11]*Dapnia, CEA Saclay, F-91191, Gif-sur-Yvette, France*
[12]*Debrecen University, H-4010 Debrecen, Egyetem tér 1, Hungary*
[13]*ELTE, Eötvös Loránd University, H - 1117 Budapest, Pázmány P. s. 1/A, Hungary*
[14]*Florida Institute of Technology, Melbourne, Florida 32901, USA*
[15]*Florida State University, Tallahassee, Florida 32306, USA*
[16]*Georgia State University, Atlanta, Georgia 30303, USA*
[17]*Hiroshima University, Kagamiyama, Higashi-Hiroshima 739-8526, Japan*
[18]*IHEP Protvino, State Research Center of Russian Federation, Institute for High Energy Physics, Protvino, 142281, Russia*
[19]*University of Illinois at Urbana-Champaign, Urbana, Illinois 61801, USA*
[20]*Institute of Physics, Academy of Sciences of the Czech Republic, Na Slovance 2, 182 21 Prague 8, Czech Republic*
[21]*Iowa State University, Ames, Iowa 50011, USA*
[22]*Joint Institute for Nuclear Research, 141980 Dubna, Moscow Region, Russia*
[23]*KEK, High Energy Accelerator Research Organization, Tsukuba, Ibaraki 305-0801, Japan*
[24]*KFKI Research Institute for Particle and Nuclear Physics of the Hungarian Academy of Sciences (MTA KFKI RMKI), H-1525 Budapest 114, PO Box 49, Budapest, Hungary*
[25]*Korea University, Seoul, 136-701, Korea*
[26]*Russian Research Center, "Kurchatov Institute", Moscow, Russia*
[27]*Kyoto University, Kyoto 606-8502, Japan*
[28]*Laboratoire Leprince-Ringuet, Ecole Polytechnique, CNRS-IN2P3, Route de Saclay, F-91128, Palaiseau, France*
[29]*Lawrence Livermore National Laboratory, Livermore, California 94550, USA*
[30]*Los Alamos National Laboratory, Los Alamos, New Mexico 87545, USA*
[31]*LPC, Université Blaise Pascal, CNRS-IN2P3, Clermont-Fd, 63177 Aubiere Cedex, France*
[32]*Department of Physics, Lund University, Box 118, SE-221 00 Lund, Sweden*
[33]*Institut für Kernphysik, University of Muenster, D-48149 Muenster, Germany*
[34]*Myongji University, Yongin, Kyonggido 449-728, Korea*
[35]*Nagasaki Institute of Applied Science, Nagasaki-shi, Nagasaki 851-0193, Japan*
[36]*University of New Mexico, Albuquerque, New Mexico 87131, USA*
[37]*New Mexico State University, Las Cruces, New Mexico 88003, USA*
[38]*Oak Ridge National Laboratory, Oak Ridge, Tennessee 37831, USA*
[39]*IPN-Orsay, Universite Paris Sud, CNRS-IN2P3, BP1, F-91406, Orsay, France*
[40]*Peking University, Beijing, People's Republic of China*
[41]*PNPI, Petersburg Nuclear Physics Institute, Gatchina, Leningrad Region, 188300, Russia*
[42]*RIKEN, The Institute of Physical and Chemical Research, Wako, Saitama 351-0198, Japan*
[43]*RIKEN BNL Research Center, Brookhaven National Laboratory, Upton, New York 11973-5000, USA*
[44]*Physics Department, Rikkyo University, 3-34-1 Nishi-Ikebukuro, Toshima, Tokyo 171-8501, Japan*
[45]*Saint Petersburg State Polytechnic University, St. Petersburg, Russia*
[46]*Instituto de Física, Universidade de São Paulo, Caixa Postal 66318, São Paulo CEP05315-970, Brazil*
[47]*System Electronics Laboratory, Seoul National University, Seoul, South Korea*
[48]*Chemistry Department, Stony Brook University, Stony Brook, SUNY, New York 11794-3400, USA*
[49]*Department of Physics and Astronomy, Stony Brook University, SUNY, Stony Brook, New York 11794, USA*
[50]*SUBATECH (Ecole des Mines de Nantes, CNRS-IN2P3, Université de Nantes), BP 20722 - 44307, Nantes, France*
[51]*University of Tennessee, Knoxville, Tennessee 37996, USA*
[52]*Department of Physics, Tokyo Institute of Technology, Oh-okayama, Meguro, Tokyo 152-8551, Japan*
[53]*Institute of Physics, University of Tsukuba, Tsukuba, Ibaraki 305, Japan*
[54]*Vanderbilt University, Nashville, Tennessee 37235, USA*
[55]*Advanced Research Institute for Science and Engineering, Waseda University, 17 Kikui-cho, Shinjuku-ku, Tokyo 162-0044, Japan*
[56]*Weizmann Institute, Rehovot 76100, Israel*

[57]Yonsei University, IPAP, Seoul 120-749, Korea
(Received 6 September 2006; published 21 December 2006)

The momentum distribution of electrons from decays of heavy flavor (charm and bottom) for midrapidity $|y| < 0.35$ in $p + p$ collisions at $\sqrt{s} = 200$ GeV has been measured by the PHENIX experiment at the BNL Relativistic Heavy Ion Collider over the transverse momentum range $0.3 < p_T < 9$ GeV/c. Two independent methods have been used to determine the heavy-flavor yields, and the results are in good agreement with each other. A fixed-order-plus-next-to-leading-log perturbative QCD calculation agrees with the data within the theoretical and experimental uncertainties, with the data/theory ratio of $1.71 \pm 0.02^{\text{stat}} \pm 0.18^{\text{sys}}$ for $0.3 < p_T < 9$ GeV/c. The total charm production cross section at this energy has also been deduced to be $\sigma_{c\bar{c}} = 567 \pm 57^{\text{stat}} \pm 193^{\text{sys}}$ μb.

DOI: 10.1103/PhysRevLett.97.252002 PACS numbers: 13.85.Qk, 13.20.Fc, 13.20.He, 25.75.Dw

Heavy-flavor (charm and bottom) production serves as a testing ground of QCD. Because of the large quark mass, it is expected that next-to-leading order perturbative QCD (NLO pQCD) can describe the production cross section of charm and bottom at high energy, particularly at high p_T. At the Tevatron, bottom production is well described by NLO pQCD [1]. Charm production cross sections at high p_T are found to be higher than the theory by $\approx 50\%$, but are compatible within the theoretical uncertainties [2]. Since heavy-flavor production at Relativistic Heavy Ion Collider (RHIC) energies is dominated by gluon-gluon fusion, its production in polarized $p + p$ collisions probes the gluon distribution $G(x)$ and the gluon polarization $\Delta G(x)$. A good understanding of the reaction mechanism for heavy-flavor production is crucial for reliably extracting these distributions. Furthermore, in Au + Au collisions at RHIC strong suppression of single electrons from heavy-flavor decays has been observed [3]. Measurements of heavy-flavor production in $p + p$ collisions provide a baseline for studying hot and dense matter effects in heavy ion reactions. Earlier measurements at RHIC [4,5] have a limited p_T range with substantial experimental uncertainties, so an improved measurement is crucial.

We report the production cross section of electrons, $(e^+ + e^-)/2$, at midrapidity in $p + p$ collisions at $\sqrt{s} = 200$ GeV for $0.3 < p_T < 9$ GeV/c measured by the PHENIX experiment. Contributions from semileptonic decays of heavy flavor are determined using two independent methods. This measurement has over 2 orders of magnitude larger statistics with much reduced systematic uncertainties compared to our previous measurement [4].

The data were collected by the PHENIX detector [6] during the 2005 RHIC run using the two central arm spectrometers. Each spectrometer covers $|\eta| < 0.35$ in pseudorapidity and $\Delta\phi = \pi/2$ in azimuth. It includes a drift chamber (DC) and pad chambers (PC1) for charged particle tracking, a ring imaging Čerenkov detector (RICH) for electron identification, and an electromagnetic calorimeter (EMCal) for electron identification and trigger. Beam-beam counters (BBCs), positioned at pseudorapidities $3.1 < |\eta| < 3.9$, measure the position of the collision vertex along the beam (z_{vtx}) and provide the interaction trigger. In this run, helium bags, one for each arm, were placed in the space between the beam pipe and DC to reduce multiple scattering and photon conversion.

Two data sets are used for the analysis: (1) the minimum bias (MB) data set recorded by the BBC trigger, and (2) a "photon" trigger (PH) data set triggered at level-1 requiring a minimum energy deposit of 1.4 GeV in an overlapping tile of 4×4 EMCal towers in coincidence with the BBC trigger. The PH trigger has $\simeq 100\%$ efficiency for high p_T electrons above 2 GeV/c in the active trigger tiles. The BBC trigger cross section is 23.0 ± 2.2 mb. Since only $\simeq 50\%$ of inelastic $p + p$ collisions satisfy the BBC trigger condition, only a fraction of the inclusive electron production events is triggered. This p_T and process independent fraction is determined to be $\epsilon_{\text{bias}} = 0.79 \pm 0.02$ from the yield ratio of high p_T π^0's with and without the BBC trigger. After selection of good runs and a vertex cut of $|z_{\text{vtx}}| < 20$ cm, an integrated luminosity ($\mathcal{L}$) of 45 nb^{-1} in the MB data set and 1.57 pb^{-1} in the PH data set are used for the analysis.

Charged particle tracks are reconstructed using DC and PC1 and confirmed by a hit in the EMCal within 4σ in position. The momentum resolution is $\sigma_p/p \simeq 0.7\% \oplus 0.9\% p$ (GeV/c), and the momentum scale is calibrated within 1% using the reconstructed mass of $J/\psi \to e^+e^-$.

Electron identification (eID) requires at least two associated hits in the RICH, a shower shape cut in the EMCal, and a cut in the ratio E/p where E is energy measured in the EMCal. We require $0.7 < E/p < 1.3$ for $0.8 < p_T < 5$ GeV/c. For lower p_T, the minimum value of E/p decreases with decreasing p_T to 0.55 at $p_T = 0.3$ GeV/c. The E/p cut removes background electrons from photon conversions and semileptonic decay of kaons ($K \to e\nu\pi(K_{e3})$) that occur far from the vertex, and most of the remaining hadron background. The hadron contamination after the E/p cut is 3% at $p_T = 0.3$ GeV/c and less than 1% for $0.8 < p_T < 5$ GeV/c with eID efficiency of approximately 90%.

For $p_T > 5$ GeV/c, where pions also emit Čerenkov photons in the RICH, tighter electron identification cuts are applied. We require at least 5 associated hits in the RICH, a tighter shower shape cut in the EMCal, and $0.8 < E/p < 1.3$. With these cuts, the electron measurement is extended to 9 GeV/c in p_T. The eID efficiency of the

tighter cuts is p_T independent, and is determined to be 57% of that for $p_T < 5$ GeV/c by applying the same tighter cuts for $p_T < 5$ GeV/c. With the tighter cuts, hadron contamination is negligible for $p_T < 7$ GeV/c. For $7 < p_T < 8 (8 < p_T < 9)$ GeV/c, a 20% (40%) hadron contamination is determined and subtracted using a Gaussian plus exponential fit to E/p distribution.

The invariant cross section for electron production is calculated using the following formula,

$$E\frac{d^3\sigma}{dp^3} = \frac{1}{\mathcal{L}}\frac{1}{2\pi p_T}\frac{N_e}{\Delta p_T \Delta y}\frac{1}{\epsilon_{\rm rec}}\frac{1}{\epsilon_{\rm bias}}, \quad (1)$$

where N_e is the measured electron yield; $\epsilon_{\rm rec}$, calculated using a full GEANT [7] simulation, includes the geometrical acceptance, track reconstruction and eID efficiency, and the smearing effect due to finite momentum resolution. For the PH data set, $\epsilon_{\rm rec}$ also includes the PH trigger efficiency. The cross sections from the MB and the PH data sets are consistent with each other for the overlapped p_T region.

The inclusive electron yield consists of three components: (1) electrons from heavy-flavor decay, (2) "photonic" background electrons from Dalitz decays of light mesons and photon conversions primarily in the beam pipe, and (3) "nonphotonic" background electrons from the remaining K_{e3} decays and dielectron decays of vector mesons. The photonic background is much larger than the nonphotonic background. We determined the spectrum of electrons from heavy-flavor decay by subtracting the background components from the inclusive spectrum using the following two independent methods.

In the "cocktail subtraction" method [3,4,8] a cocktail of electron spectra from various background sources is calculated using a Monte Carlo event generator of hadron decays. The most important background is the π^0 Dalitz decay, so we use our measured π^0 and $\pi^\pm$ spectra as input to the generator. The spectral shapes of other light hadrons h are obtained from the pion spectra by m_T scaling ($p_T \rightarrow \sqrt{p_T^2 + M_h^2 - M_\pi^2}$). Within this approach the ratios h/π^0 are constant at high p_T. For the relative normalization, we use the following ratios: $\eta/\pi^0 = 0.48 \pm 0.03$ [9], $\rho^0/\pi^0 = 1.0 \pm 0.3$, $\omega/\pi^0 = 0.90 \pm 0.06$ [10], $\eta'/\pi^0 = 0.40 \pm 0.12$, $\phi/\pi^0 = 0.25 \pm 0.08$. For $p_T > 2$ GeV/c, contributions from η and all other hadrons combined are approximately 20% and 10% of π^0, respectively. Another major background electron source is conversions of photons in the beam pipe [0.29% of a radiation length (X_0)] as well as in the air and the helium bags (0.1% X_0). The conversion electron spectrum is very similar to that of Dalitz decays. Using a detailed GEANT simulation of the PHENIX detector, the ratio of electrons from conversions to Dalitz decays, $R_{\rm CD}$, is determined to be 0.40 ± 0.04 for π^0, essentially p_T independent. $R_{\rm CD}$ is approximately half of that in [4] since the helium bags eliminated most of the conversions outside of the beam pipe. The conversion spectra are calculated by scaling the Dalitz decay spectra by $R_{\rm CD}$, with small corrections to account for the species dependence of the relative branching ratio of Dalitz decay to photon decay [$(h \rightarrow ee\gamma)/(h \rightarrow \gamma\gamma)$]. The internal and external conversions of direct photons are also included in the cocktail, using our measured direct photon spectrum [11] as input. The direct photon contribution is comparable to or greater than that from the η for $p_T > 5$ GeV/c. Nonphotonic backgrounds are also included in the cocktail. Since the K_{e3} background depends on the analysis cuts, it is evaluated by a full GEANT simulation.

In the "converter subtraction" method [12], we introduce an additional photon converter (a thin brass sheet of 1.67% X_0) around the beam pipe for part of the run. The converter multiplies the photonic electron background by a fixed factor, $R_\gamma \simeq 2.3$, which is determined precisely via GEANT simulation. R_γ is larger than in [12] since we have less conversion material in the 2005 run. The photonic background N_e^γ is determined as $N_e^\gamma = [N_e^C - (1-\epsilon)N_e^{\rm NC}]/(R_\gamma - 1 + \epsilon)$, where N_e^C and $N_e^{\rm NC}$ are electron yield with and without the converter, respectively, and ϵ (2.1%) represents a small loss of electrons due to the converter. The nonphotonic component is then determined as $N_e^{\rm non\text{-}\gamma} = N_e^{\rm NC} - N_e^\gamma$. Small remaining nonphotonic backgrounds, such as K_{e3} and hadron contamination, are subtracted.

These two methods are complementary to each other. The converter method is more accurate, and it allows us to extract a heavy-flavor signal down to $p_T = 0.3$ GeV/c where the signal is only $\approx 10\%$ of inclusive electrons. In addition, the measured photonic background N_e^γ is used to confirm and to calibrate the normalization of the calculated cocktail yields. A drawback of the method is statistical precision: the converter run contains only a small fraction ($\simeq$7% in the 2005 run) of the data. The cocktail method can use the full statistics at high p_T, where the photonic background becomes a small fraction of inclusive electrons.

Systematic uncertainties are categorized into (a) inclusive electron spectra, (b) cocktail subtraction, and (c) converter subtraction. Category (a) is common to both analyses, and includes the uncertainties in luminosity (9.6%), geometrical acceptance (4%), eID efficiency (3%), and the PH trigger efficiency (3% at the plateau). Uncertainties in cocktail subtraction [category (b)] include the normalization (8%) and p_T dependent shape uncertainty (2% at $p_T \simeq 2$ GeV/c, increasing to 6% at 9 GeV/c). In the converter analysis [category (c)] the dominant uncertainties are in R_γ (2.7%) and in the relative acceptance in the converter and the normal runs (1.0%). These uncertainties are propagated into the uncertainties in the heavy-flavor electron yields and added in quadrature.

Figure 1 shows the ratio of the measured N_e^γ to the cocktail calculation as a function of p_T. The ratio is consistent with unity within the uncertainties of the cocktail. At high p_T (>1.8 GeV/c), the ratio is $0.94 \pm 0.02^{\rm stat}$ on average. Since this is within the uncertainty of the cocktail

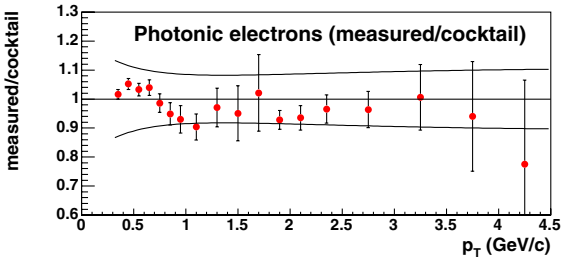

FIG. 1 (color online). Ratio of photonic electrons measured by the converter method to the cocktail calculation. Data from the MB (PH) data set are shown below (above) 1.8 GeV/c. The upper and lower curves show the systematic error of the cocktail. Error bars are statistical only.

normalization, we rescale the cocktail yields by this factor. This removes the 8% normalization uncertainty in the cocktail.

In Fig. 2, filled circles (squares) show the ratio of nonphotonic electrons relative to photonic background determined by the converter (cocktail) method. The nonphotonic electrons are dominantly heavy-flavor decay signals. The remaining nonphotonic background contributions have been calculated and are shown in Fig. 2. The two methods are consistent with each other. The ratio monotonically increases with increasing p_T, becoming greater than unity for $p_T > 2.4$ GeV/c, and saturates at $\simeq 3$ for $p_T > 5$ GeV/c. The large signal-to-background ratio is due to the small amount of conversion material in the spectrometer acceptance.

Figure 3(a) shows the invariant differential cross section of electrons from heavy-flavor decays. All background has been subtracted, including the nonphotonic components shown in Fig. 2. The data from the two analysis methods

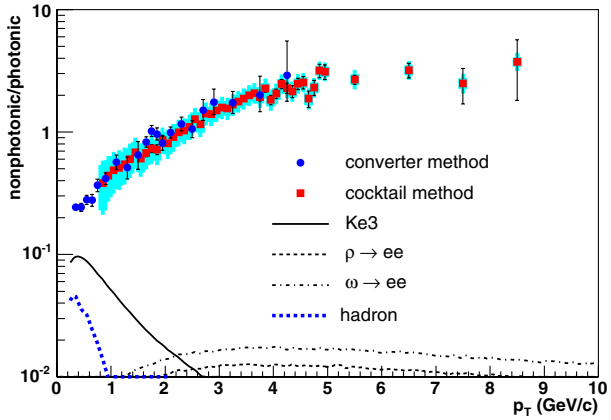

FIG. 2 (color online). Ratio of nonphotonic electrons to photonic background. Error bars are statistical errors and the error bands show the cocktail systematic errors. The solid, dashed, dot-dashed, and dot curve are the remaining nonphotonic backgrounds from K_{e3}, $\rho \rightarrow ee$, $\omega \rightarrow ee$, and hadron contamination, respectively.

are combined: at low p_T ($p_T < 1.6$ GeV/c) the converter subtraction method on the MB data set is used; at intermediate p_T ($1.6 < p_T < 2.6$ GeV/c) the converter method on the PH data set is used; and at high p_T ($p_T > 2.6$ GeV/c) the cocktail method on the PH data set is used.

The data are compared with a fixed-order-plus-next-to-leading-log (FONLL) pQCD calculation [13,14]. The top curve in Fig. 3 shows the central values of the FONLL calculation. The contributions of charm and bottom are also shown. For $p_T > 4$ GeV/c, the bottom contribution becomes dominant. In Fig. 3(b), the ratio of the data to the FONLL calculation is shown. The ratio is nearly p_T independent over the entire p_T range. Fitting to a constant for $0.3 < p_T < 9.0$ GeV/c yields a ratio of $1.71 \pm 0.02^{\text{stat}} \pm 0.18^{\text{sys}}$. Similar ratios are observed in charm production at high p_T at the Tevatron [2]. The upper limit of the FONLL calculation is compatible with the data. Recently STAR also reported nonphotonic electron production in $p + p$ at $\sqrt{s} = 200$ GeV [15].

The total charm cross section is derived by integrating the heavy-flavor electron cross section for $p_T > 0.4$ GeV/c: $d\sigma_e(p_T > 0.4)/dy = 5.95 \pm 0.59^{\text{stat}} \pm 2.0^{\text{sys}}$ μb. The systematic error is obtained by integrating the upper and lower systematic error limits of the differential cross sections, since the systematic errors are essentially coherent. The cross section is then extrapolated to

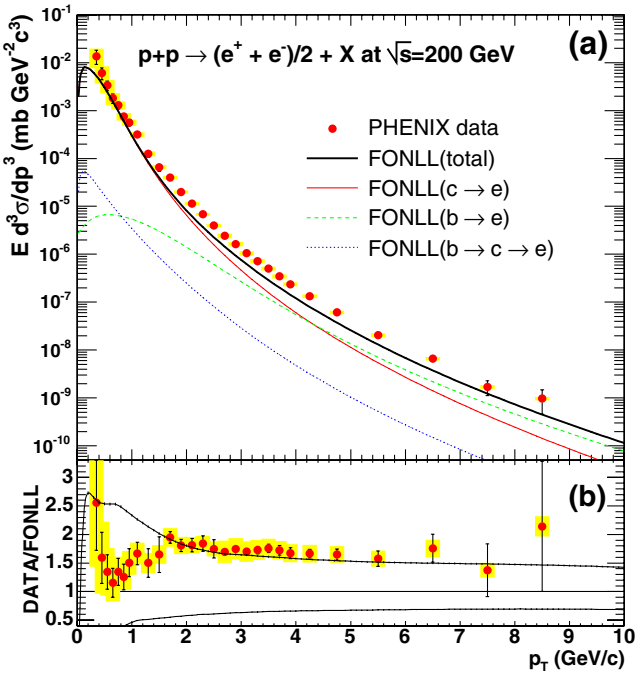

FIG. 3 (color online). (a) Invariant differential cross sections of electrons from heavy-flavor decays. The error bars (bands) represent the statistical (systematic) errors. The curves are the FONLL calculations (see text). (b) Ratio of the data and the FONLL calculation. The upper (lower) curve shows the theoretical upper (lower) limit of the FONLL calculation. In both panels a 10% normalization uncertainty is not shown.

$p_T = 0$ using the spectrum shape predicted by FONLL: $d\sigma_e(p_T > 0)/dy = 10.9 \pm 1.1^{\text{stat}} \pm 3.1^{\text{sys}}$ μb. We have assigned 10% to the systematic uncertainty of the extrapolation, and have subtracted contribution from bottom and bottom cascade decays (0.1 μb). We determine the charm production cross section, $d\sigma_{c\bar{c}}/dy = 123 \pm 12^{\text{stat}} \pm 37^{\text{sys}}$ μb, by using a $c \rightarrow e$ total branching ratio of $9.5 \pm 1.0\%$, calculated using the following charmed hadron ratios: $D^+/D^0 = 0.45 \pm 0.1$, $D_s/D^0 = 0.25 \pm 0.1$, and $\Lambda_c/D^0 = 0.1 \pm 0.05$. The rapidity distribution of electrons is broader than that of D mesons due to decay kinematics. A correction to this effect (7%) has been applied. Using the rapidity distribution from HVQMNR [16] with CTEQ5M [17] PDF, the total charm cross section is determined to be $\sigma_{c\bar{c}} = 567 \pm 57^{\text{stat}} \pm 193^{\text{sys}}$ μb. We have assigned 15% systematic error to the extrapolation. This result is compatible with our previous measurement [4] ($920 \pm 150^{\text{stat}} \pm 540^{\text{sys}}$ μb) and the value derived from Au + Au collisions [12] ($622 \pm 57^{\text{stat}} \pm 160^{\text{sys}}$ μb per NN collision). The FONLL cross section (256^{+400}_{-146} μb) is compatible with the data within its uncertainty. STAR has reported a somewhat larger value in d + Au [5] ($1.3 \pm 0.2^{\text{stat}} \pm 0.4^{\text{sys}}$ mb per NN collisions). Although the data extend to high p_T where the bottom contribution is expected to be dominant, the present analysis does not separate charm and bottom contributions. The bottom cross section predicted by FONLL is $1.87^{+0.99}_{-0.67}$ μb, and the upper FONLL curve is consistent with the data.

In conclusion, we have measured single electrons from heavy-flavor decays in $p + p$ collisions at $\sqrt{s} = 200$ GeV. The new data reported here provide a crucial baseline for the study of heavy quark production in hot and dense matter created in Au + Au collisions. The agreement between the data and the FONLL pQCD calculation within the theoretical and the experimental uncertainties suggests that a reliable extraction of gluon polarization from heavy-flavor production in polarized $p + p$ collisions is attainable.

We thank the staff of the Collider-Accelerator and Physics Departments at BNL for their vital contributions. We acknowledge support from the Department of Energy and NSF (USA), MEXT and JSPS (Japan), CNPq and FAPESP (Brazil), NSFC (China), MSMT (Czech Republic), IN2P3/CNRS, and CEA (France), BMBF, DAAD, and AvH (Germany), OTKA (Hungary), DAE (India), ISF (Israel), KRF and KOSEF (Korea), MES, RAS, and FAAE (Russia), VR and KAW (Sweden), US CRDF for the FSU, US-Hungarian NSF-OTKA-MTA, and US-Israel BSF.

*Deceased.
†PHENIX Spokesperson.
Email address: zajc@nevis.columbia.edu

[1] M. Cacciari, hep-ph/0407187.
[2] D. Acosta *et al.*, Phys. Rev. Lett. **91**, 241804 (2003).
[3] S. S. Adler *et al.*, Phys. Rev. Lett. **96**, 032301 (2006).
[4] S. S. Adler *et al.*, Phys. Rev. Lett. **96**, 032001 (2006).
[5] J. Adams *et al.*, Phys. Rev. Lett. **94**, 062301 (2005).
[6] K. Adcox *et al.*, Nucl. Instrum. Methods Phys. Res., Sect. A **499**, 469 (2003).
[7] F. Carminati *et al.*, *GEANT 3.21: Detector Description and Simulation Tool*, CERN Program Library Long Writeup W5013, 1993.
[8] K. Adcox *et al.*, Phys. Rev. Lett. **88**, 192303 (2002).
[9] S. S. Adler *et al.*, Phys. Rev. Lett. **96**, 202301 (2006).
[10] V. Ryabov *et al.*, Nucl. Phys. **A774**, 735 (2006).
[11] S. S. Adler *et al.*, hep-ex/0609031 [Phys. Rev. Lett. (to be published)].
[12] S. S. Adler *et al.*, Phys. Rev. Lett. **94**, 082301 (2005).
[13] M. Cacciari, P. Nason, and R. Vogt, Phys. Rev. Lett. **95**, 122001 (2005).
[14] M. Cacciari (private communication).
[15] B. I. Abelev *et al.* (STAR Collaboration), nucl-ex/0607012.
[16] M. L. Mangano, P. Nason, and G. Ridolfi, Nucl. Phys. **B405**, 507 (1993).
[17] H. L. Lai *et al.*, Eur. Phys. J. C **12**, 375 (2000).